

# Far Field measurement in the focal plane of a lens : a cautionary note

Pierre Suret and Stéphane Randoux

Laboratoire de Physique des Lasers, Atomes et Molécules, UMR CNRS 8523,  
Université Lille 1, Sciences et Technologies, F-59655 Villeneuve d'Ascq, France

[Pierre.Suret@univ-lille1.fr](mailto:Pierre.Suret@univ-lille1.fr)

## Abstract:

We study theoretically the accuracy of the method based on the Fourier property of lenses that is commonly used for the far field measurement. We consider a simple optical setup in which the far-field intensity pattern of a light beam passing through a Kerr medium is recorded by a CCD camera located in the back focal plane of a thin lens. Using Fresnel diffraction formula and numerical computations, we investigate the influence of a slight longitudinal mispositioning of the CCD camera. Considering a coherent gaussian beam, we show that a tiny error in the position of the CCD camera can produce a narrowing of the transverse pattern instead of the anticipated and well-understood broadening. This phenomenon is robust enough to persist for incoherent beams strongly modified by the presence of noise. The existence of this phenomenon has important consequences for the design and the realization of experiments in the field of optical wave turbulence in which equilibrium spectra reached by incoherent waves can only be determined from a careful far-field analysis. In particular, the unexpected narrowing of the far field may be mistaken for the remarkable phenomenon of classical condensation of waves. Finally, we show that the finite-size of optical components used in experiments produces diffraction patterns having wings decaying in a way comparable to the Rayleigh-Jeans distribution reached by incoherent wave systems at thermodynamical equilibrium.

---

## References and links

1. A. Porter, "On the diffraction theory of microscopic vision," *Phil. Mag.* **11**, 154 (1906).
2. J. Goodman, *Introduction to Fourier Optics* (Roberts & Co Publishers, 2005), third edition ed.
3. P. Elias, D. Grey, and D. Robinson, "Fourier treatment of optical processes," *J. Opt. Soc. Am.* **42**, 127–132 (1952).
4. P. Elias, "Optics and communication theory," *J. Opt. Soc. Am.* **43**, 229–232 (1953).
5. P.-M. Duffieux, *The Fourier Transform and its Applications to Optics* (Wiley, New York, 1983).
6. J. Rhodes, "Analysis and synthesis of optical images," *Am. J. Phys* **21**, 337 (1953).
7. W. Gambling, D. Payne, H. Matsumura, and R. Dyott, "Determination of core diameter and refractive-index difference of single-mode fibres by observation of the far-field pattern," *IEEE Journal on Microwaves, Optics and Acoustics* **1**, 13–17 (1976).
8. K. Hotate and T. Okoshi, "Measurement of refractive-index profile and transmission characteristics of a single-mode optical fiber from its exit-radiation pattern," *Appl. Opt.* **18**, 3265–3271 (1979).
9. P. J. Samson, "Measurement of wavelength dependence of the far-field pattern of single-mode optical fibers," *Opt. Lett.* **10**, 306–308 (1985).
10. W. Freude and A. Sharma, "Refractive-index profile and modal dispersion prediction for a single-mode optical waveguide from its far-field radiation pattern," *Journal of Lightwave Technology* **3**, 628–634 (1985).
11. W. Callen, B. Huth, and R. Pantell, "Optical patterns of thermally self-defocused light," *Appl. Phys. Lett.* **11**, 103 (1967).

12. C. Nascimento, M. Alencar, S. Chavez-Cerda, M. da Silva, M. Meneghetti, and J. Hickmann, "Experimental demonstration of novel effects on the far-field diffraction patterns of a gaussian beam in a kerr medium," *Journal of Optics A: Pure and Applied Optics* **8**, 947 (2006).
13. T. Wulle and S. Herminghaus, "Nonlinear optics of bessel beams," *Phys. Rev. Lett.* **70**, 1401–1404 (1993).
14. T. Honda, H. Matsumoto, M. Sedlatschek, C. Denz, and T. Tschudi, "Spontaneous formation of hexagons, squares and squeezed hexagons in a photorefractive phase conjugator with virtually internal feedback mirror," *Optics Communications* **133**, 293 – 299 (1997).
15. C. Denz, M. Schwab, M. Sedlatschek, T. Tschudi, and T. Honda, "Pattern dynamics and competition in a photorefractive feedback system," *J. Opt. Soc. Am. B* **15**, 2057–2064 (1998).
16. E. O'Neill, J. Houlihan, J. G. McInerney, and G. Huyet, "Dynamics of traveling waves in the transverse section of a laser," *Phys. Rev. Lett.* **94**, 143901 (2005).
17. von F. Zernike, "Beugungstheorie des schneidenverfahrens und seiner verbesserten form, der phasenkontrastmethode," *Physica* **1**, 689 – 704 (1934).
18. F. Zernike, "How i discovered phase contrast," *Science* **121**, 345–349 (1955).
19. L. Lucchetti, S. Suchand, and F. Simoni, "Fine structure in spatial self-phase modulation patterns: at a glance determination of the sign of optical nonlinearity in highly nonlinear films," *J. Opt. A: Pure Appl. Opt.* **11**, 034002 (2009).
20. M. M. Birky, "Simultaneous recording of near-field and far-field patterns of lasers," *Appl. Opt.* **8**, 2249–2253 (1969).
21. M. Cross and P. Hohenberg, "Pattern formation outside of equilibrium," *Reviews of modern physics* **65**, 851 (1993).
22. N. B. Abraham and W. J. Firth, "Overview of transverse effects in nonlinear-optical systems," *J. Opt. Soc. Am. B* **7**, 951–962 (1990).
23. F. Arecchi, S. Boccaletti, and P. Ramazza, "Pattern formation and competition in nonlinear optics," *Physics Reports* **318**, 1 – 83 (1999).
24. E. Große Westhoff, R. Herrero, T. Ackemann, and W. Lange, "Self-organized superlattice patterns with two slightly differing wave numbers," *Phys. Rev. E* **67**, 025203 (2003).
25. C. Denz, M. Schwab, and C. Weillau, *Transverse-Pattern Formation in Photorefractive Optics*, Springer Tracts in Modern Physics (Springer, 2003).
26. F. Arecchi, "Optical morphogenesis : pattern formation and competition in nonlinear optics," *Physica D* **86**, 297–322 (1995).
27. P. Ramazza, E. Pampaloni, S. Residori, and F. Arecchi, "Optical pattern formation in a kerr-like medium with feedback," *Physica D: Nonlinear Phenomena* **96**, 259 – 271 (1996).
28. P. Ramazza, S. Boccaletti, and F. Arecchi, "Transport induced patterns in an optical system with focussing nonlinearity," *Optics Communications* **136**, 267 – 272 (1997).
29. G. Agez, P. Glorieux, C. Szwaj, and E. Louvergneaux, "Using noise speckle pattern for the measurements of director reorientational relaxation time and diffusion length of aligned liquid crystals," *Optics Communications* **245**, 243 – 247 (2005).
30. G. Agez, P. Glorieux, M. Taki, and E. Louvergneaux, "Two-dimensional noise-sustained structures in optics: Theory and experiments," *Phys. Rev. A* **74**, 043814 (2006).
31. S. Gentilini, N. Ghofraniha, E. DelRe, and C. Conti, "Shock wave far-field in ordered and disordered nonlocal media," *Opt. Express* **20**, 27369–27375 (2012).
32. M. Kolesik, E. M. Wright, and J. V. Moloney, "Interpretation of the spectrally resolved far field of femtosecond pulses propagating in bulk nonlinear dispersive media," *Opt. Express* **13**, 10729–10741 (2005).
33. D. Faccio, A. Averbchi, A. Lotti, P. D. Trapani, A. Couairon, D. Papazoglou, and S. Tzortzakis, "Ultrashort laser pulse filamentation fromspontaneous xwave formation in air," *Opt. Express* **16**, 1565–1570 (2008).
34. W. Wan, S. Jia, and J. W. Fleischer, "Dispersive superfluid-like shock waves in nonlinear optics," *Nature Physics* **3**, 46–51 (2007).
35. V. Zakharov, V. L'vov, and G. Falkovich, *Kolmogorov Spectra of Turbulence I*, Berlin (Springer, 1992).
36. A. Newell and R. B., "Wave turbulence," *Annual review of Fluid Mechanics* **43**, 59–78 (2011).
37. B. Miquel and N. Mordant, "Nonstationary wave turbulence in an elastic plate," *Phys. Rev. Lett.* **107**, 034501 (2011).
38. A. Picozzi, "Towards a nonequilibrium thermodynamic description of incoherent nonlinear optics," *Opt. Express* **15**, 9063 (2007).
39. C. Connaughton, C. Josserand, A. Picozzi, Y. Pomeau, and S. Rica, "Condensation of classical nonlinear waves," *Phys. Rev. Lett.* **95**, 263901 (2005).
40. S. Dyachenko, A. C. Newell, A. Pushkarev, and V. E. Zakharov, "Optical turbulence: weak turbulence, condensates and collapsing filaments in the nonlinear schrödinger equation," *Physica D* **57**, 96 (1992).
41. S. Pitois, S. Lagrange, H. R. Jauslin, and A. Picozzi, "Velocity locking of incoherent nonlinear wave packets," *Phys. Rev. Lett.* **97**, 033902 (2006).
42. B. Barviau, S. Randoux, and P. Suret, "Spectral broadening of a multimode continuous-wave optical field propagating in the normal dispersion regime of a fiber," *Opt. Lett.* **31**, 1696 (2006).

43. B. Barviau, B. Kibler, A. Kudlinski, A. Mussot, G. Millot, and A. Picozzi, "Towards a nonequilibrium thermodynamic description of incoherent nonlinear optics," *Opt. Express* **15**, 9063 (2009).
44. P. Suret, S. Randoux, H. Jauslin, and A. Picozzi, "Anomalous thermalization of nonlinear wave systems," *Phys. Rev. Lett.* **104**, 054101 (2010).
45. P. Suret, A. Picozzi, and S. Randoux, "Wave turbulence in integrable systems: nonlinear propagation of incoherent optical waves in single-mode fibers," *Opt. Express* **19**, 17852–17863 (2011).
46. U. Bortolozzo, J. Laurie, S. Nazarenko, and S. Residori, "Optical wave turbulence and the condensation of light," *J. Opt. Soc. Am. B* **26**, 2280–2284 (2009).
47. J. Laurie, U. Bortolozzo, S. Nazarenko, and S. Residori, "One-dimensional optical wave turbulence: Experiment and theory," *Physics Reports* **514**, 121 – 175 (2012).
48. C. Sun, S. Jia, C. Barsi, S. Rica, A. Picozzi, and J. W. Fleischer, "Observation of the kinetic condensation of classical waves," *Nature Physics* **8**, 470–474 (2012).
49. S. Durbin, S. Arakelian, and Y. Shen, "Laser-induced diffraction rings from a nematic-liquid-crystal film," *Opt. Lett.* **6**, 411 (1981).
50. F. Dabby, T. Gustafson, J. Whinnery, and Y. Kohanzadeh, "Thermally self-induced phase modulation of laser beams," *Appl. Phys. Lett.* **16**, 362 (1970).
51. E. Santamato and Y. Shen, "Field-curvature effect on the diffraction ring pattern of a laser beam dressed by spatial self-phase modulation in a nematic film," *Opt. Lett.* **9**, 564 (1984).
52. L. Deng, K. He, T. Zhou, and C. Li, "Formation and evolution of far-field diffraction patterns of divergent and convergent gaussian beams passing through self-focusing and self-defocusing media," *Journal of Optics A: Pure and Applied Optics* **7**, 409 (2005).
53. E. V. G. Ramirez, M. L. A. Carrasco, M. M. M. Otero, S. C. Cerda, and M. D. I. Castillo, "Far field intensity distributions due to spatial self phase modulation of a gaussian beam by a thin nonlocal nonlinear media," *Opt. Express* **18**, 22067–22079 (2010).
54. R. W. Boyd, *Nonlinear Optics* (Academic Press, 1992).
55. J. Castillo, V. P. Kozich, and A. M. O., "Thermal lensing resulting from one- and two-photon absorption studied with a two-color time-resolved z scan," *Opt. Lett.* **19**, 171–173 (1994).
56. R. E. Samad and J. Nilson Dias Vieira, "Analytical description of z-scan on-axis intensity based on the Huygens–Fresnel principle," *J. Opt. Soc. Am. B* **15**, 2742–2747 (1998).
57. I. C. Khoo, J. Y. Hou, T. H. Liu, P. Y. Yan, R. R. Michael, and G. M. Finn, "Transverse self-phase modulation and bistability in the transmission of a laser beam through a nonlinear thin film," *J. Opt. Soc. Am. B* **4**, 886–891 (1987).
58. M. Sheik-bahae, A. A. Said, and E. W. V. Stryland, "High-sensitivity, single-beam  $n_2$  measurements," *Opt. Lett.* **14**, 955–957 (1989).
59. M. Sheik-Bahae, A. Said, T.-H. Wei, D. Hagan, and E. V. Stryland, "Sensitive measurement of optical nonlinearities using a single beam," *Journal of Quantum Electronics*, *IEEE* **26**, 760–769 (1990).
60. L. Deng, K. He, T. Zhou, and C. Li, "Formation and evolution of far-field diffraction patterns of divergent and convergent gaussian beams passing through self-focusing and self-defocusing media," *Journal of Optics A: Pure and Applied Optics* **7**, 409 (2005).
61. M. Frigo and S. G. Johnson, "The design and implementation of FFTW3," *Proceedings of the IEEE* **93**, 216–231 (2005). Special issue on "Program Generation, Optimization, and Platform Adaptation".

## 1. Introduction

More than one century ago, experiments made by Abbe and Porter provided the first spatial Fourier analysis of an object by observing the transmitted light in the focal plane of a lens [1, 2]. From these pioneering works, Fourier optics theory has been widely used to describe the propagation of light through lenses, to determine the resolution of optical instruments and to elaborate image processing techniques [2–5]. Fourier optics is based on the Fourier transform property of lenses : the electric field in the back focal plane is the Fraunhofer diffraction pattern *i.e.* the Fourier transform of the electric field profile in the front focal plane [2, 6].

In the paraxial approximation, the Fraunhofer diffraction pattern corresponds to the so-called far-field profile, *i.e.* the intensity profile observed very far away from the source. In optical experiments, the far-field pattern may be measured without any lens. For instance, the far field pattern at the output of optical fibers can be simply measured with a single point detector rotating on a circle having its center that coincides with the output end of the fiber [7–10]. Another approach has been used in some nonlinear optical experiments in which far field patterns of laser fields modified by nonlinear interactions have been directly observed on screens or cam-

eras placed far from the nonlinear medium. [11–16].

However observation of the Fraunhofer pattern in the focal plane of a thin lens provides a simple finite-distance method for the exact measurement of the Fourier spectral power density. Placing amplitude or phase masks in the focal plane of the lens, manipulation of the transverse characteristics of light beams can be additionally implemented [2, 17, 18].

Nowadays the measurement of the far-field is widely used in various areas of optical research. In particular, measurements of the far field intensity pattern can be used to determine some linear and nonlinear properties of optical materials. For instance the transverse index profile of optical fibers can be determined from a far field analysis [7, 8, 10]. The sign of Kerr coefficient of nonlinear materials can be determined from simple visualisations of the far-field pattern of a gaussian beam passing through the nonlinear sample [19].

Beyond those conceptually simple measurements of optical properties, the far-field pattern plays an important role in nonlinear optics since it represents a major tool to investigate complex spatiotemporal phenomena. In particular, (transverse) phase matching conditions that deeply influence nonlinear interactions such as second harmonic generation can be precisely studied from far-field observations [13]. In this context, the observation of the far-field pattern is often considered as a complementary tool of the observation of the near-field pattern, especially regarding lasers systems [20].

In the field of nonlinear dynamics, the concept of far-field is widely used in theoretical and experimental studies of transverse pattern formation [21]. Over the last thirty years, far-field observation has been extensively used to investigate pattern formation in nonlinear optical systems based on photorefractive or liquid crystals [14, 22–31]. Let us emphasize that far-field determination is not only used for static patterns but it can also be very useful to analyse complex spatio-temporal behavior occurring in X-waves formation, filamentation phenomena [32, 33] or dispersive shock waves [31, 34].

Optical wave turbulence has recently emerged as a field in which the experimental determination of the transverse far-field pattern is of crucial importance. Wave turbulence (WT) can be defined as the non-equilibrium statistical dynamics of ensembles of nonlinearly-interacting dispersive waves [35]. The archetype of wave turbulence is the random state of ocean surfaces but it appears in various systems involving *e.g.* capillary waves, plasma waves, or elastic waves [36, 37].

Recently, nonlinear optical (in particular Kerr-like) systems have turned out to be used for the investigation of wave turbulence [38–40]. Several experimental studies of wave turbulence and wave thermalization of incoherent waves have been achieved in 1D systems based on optical fibers [41–45] and liquid crystals [46, 47].

In Hamiltonian systems (described for instance by 2D or 3D Nonlinear Schrödinger equations) WT theory predicts the existence of a state of thermodynamical equilibrium associated with a (kinetic) energy equipartition among the Fourier components of the transverse field. The thermodynamical equilibrium distribution reached by the wave system is named the Rayleigh-Jeans distribution. It is characterized by a lorentzian Fourier spectrum decaying according to a power law  $k^{-2} = |\mathbf{k}|^{-2}$  for high-frequency wavenumbers  $\mathbf{k}$  observed in the far-field [35, 38, 41]. Additionally, the thermodynamical equilibrium of nonlinear incoherent waves may exhibit a phenomenon of (classical) *wave condensation* analog to the Bose-Einstein condensation of atoms [39, 40]. The main signature of this condensation process is the accumulation of (quasi-) particles in the fundamental Fourier component  $\mathbf{k} \sim \mathbf{0}$ . The observation of the thermodynamical equilibrium distribution and of the process of wave condensation represents currently an experimental challenge in fundamental physics.

Sun *et al.* have very recently studied the propagation of 2D incoherent waves interacting in a Kerr-like photorefractive crystal [48]. In particular they report the observation of far-field intensity patterns measured with a camera placed in the focal plane of a lens. When the strength of the nonlinearity is increased, Sun *et al.* have observed accumulation of light around the transverse wavevector of lowest value ( $\mathbf{k} \sim \mathbf{0}$  and its transverse coordinates  $k_x \sim 0$  and  $k_y \sim 0$ ) and they have interpreted this observation as the phenomenon of optical wave condensation. Recording the far-field intensity pattern over four decades, they report a high-dynamic measurement in which they evidence a spectrum decaying over more than three decades according to a power law of  $k_x^{-2}$ . The authors interpret the observation of this power law as the Rayleigh-Jeans distribution, a signature of thermodynamical equilibrium of the optical waves [48].

In those incoherent nonlinear optical experiments, proofs of the existence of the phenomena of wave condensation and thermalization can only be achieved from the measurement of the far-field transverse intensity pattern. In this paper, we investigate questions related to the existence of some experimental uncertainties that necessarily arise in the measurement of the far-field intensity pattern in the focal plane of a lens. We focus on the measurement of transverse spectrum (wavevectors) of a gaussian beam passing through a Kerr-like medium. We show in particular that the far-field pattern dramatically depends on the position of the observation screen (or camera). Our main results concern the observation of the far-field in a plane very close to (but not exactly in) the focal plane of the lens. When the third order nonlinearity increases, we show from numerical simulations that the observed far-field can narrow whereas the true far-field measured exactly in the focal plane broadens. This phenomenon can lead to serious misinterpretations of the observations made in optical turbulence experiments.

In Sec. 2, we describe the typical experiments in which the far field of light passing through a thin Kerr medium is observed nearby the focal plane of a thin lens. We recall the usual and simple theoretical description of light propagation in the setup under consideration [2]. In Sec. 3, we present the main result of this paper. Using the Fresnel diffraction formula, we compute the far-field pattern of a coherent gaussian beam passing through a thin Kerr-like medium. As it is well-known, the Fourier spectrum monotonically broadens with concentric rings when the strength of the Kerr effect increases [11, 12, 49–53]. This is actually what is obtained from numerical simulations but observing the transverse pattern in a plane slightly shifted from the focal plane, we contrarily observe a narrowing of the transverse pattern instead of a broadening. In Sec. 4, we show that this phenomenon persists for an initially incoherent beam. This means that experiments on optical wave condensation are dramatically sensitive to the alignment of the experimental setup. In Sec. 5, we show that light diffraction by the edges of the nonlinear crystal can also lead to a misinterpretation of power laws experimentally observed in the Fourier spectrum.

## 2. Position of the problem

In this article we consider a conceptually-simple setup found in many nonlinear optical experiments : the far-field of a light beam passing through a Kerr medium is measured in the focal plane of a thin lens [26–28, 48]. Fig. 1 represents a typical scheme of the setup under consideration.

The light beam propagating along the  $z$ -axis is supposed to be monochromatic and linearly-polarized. It is associated to an electric field  $E$  that reads:

$$E(x, y, z, t) = A(x, y, z) e^{j(k_0 z - \omega_0 t)} \quad (1)$$

$A(x, y, z)$  is the complex amplitude of the field that is supposed to be a slowly-varying function of the longitudinal coordinate  $z$ .  $k_0 = \omega_0/c = 2\pi/\lambda$  is the wavenumber,  $c$  is the speed of light in vacuum and  $\lambda$  is the wavelength of the electric field in vacuum. In all the computations presented in this paper, the numerical value taken for the wavelength  $\lambda$  is 532 nm.

The light beam passes through a transparent Kerr medium having a length  $L$ . In our discussion, the exact nature of this Kerr medium has only little importance : it can be either a piece of bulk silica, a liquid crystal layer or a photorefractive crystal [54]. The nonlinear effect under consideration can be either focusing or defocusing. The transverse field incident onto the entrance side of the Kerr medium is  $A(x, y, z = -L) = A_{in}(x, y)$ . The transverse field found at the output side of the Kerr medium is  $A(x, y, z = 0) = A_0(x', y')$  (see Fig. 1).

Let us consider that we want to record the transverse far-field pattern of the field  $A_0(x, y)$  by using the standard and simple setup shown in Fig. 1. Let us recall that the so-called *far field*  $n(k_x, k_y)$  is the spectral power density of  $A_0(x, y)$ . It is simply defined as

$$n(k_x, k_y) = \left| \widetilde{A}_0(k_x, k_y) \right|^2 \quad (2)$$

where the transverse Fourier Transform (FT) of the amplitude  $A_0(x, y)$  is defined by:

$$FT\left(A_0(x, y)\right) = \widetilde{A}_0(k_x, k_y) = \int \int_{-\infty}^{+\infty} A_0(x, y) e^{-i(k_x x + k_y y)} dx dy \quad (3)$$

In order to measure the far-field pattern, the light beam passes through a perfectly stigmatic thin lens having a focal length  $f'$  and adding a power-independent quadratic term to the transverse phase of  $A_0(x, y)$ . The intensity profile  $|A_d(x, y)|^2$  is observed with a camera in the plane  $(O, x, y)$ . As shown in Fig. 1,  $d_0$  is the distance between the output side of the Kerr medium and the thin lens whereas  $d$  is the distance between the thin lens and the camera.

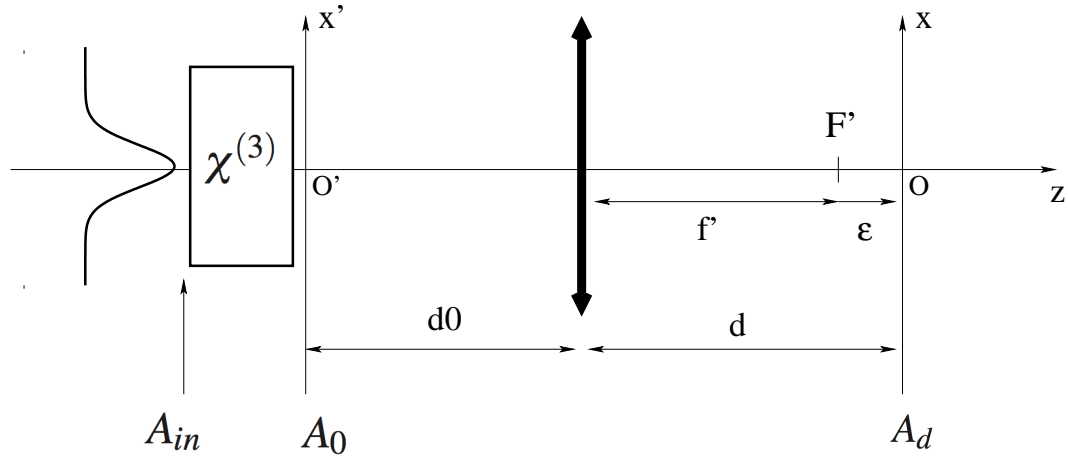


Fig. 1. *Experimental setup.* The incident field  $A_{in}(x, y)$  passes through a thin Kerr  $(\chi^{(3)})$  medium.  $A_0(x', y')$  is the field in the output plane  $(O'x'y')$  of the  $\chi^{(3)}$  medium. In order to measure the far-field of  $A_0(x', y')$ , the light propagates through a positive thin lens with a focal length  $f'$ .  $d_0$  is the distance between the plane  $(O'x'y')$  and the lens. The transverse intensity profile  $|A_d(x, y)|^2$  is observed in a plane close to the focal plane of the lens :  $d = f' + \epsilon$  is the distance between the lens and the observation plane  $(Oxy)$ .

Let us briefly recall why the transverse profile  $|A_d(x, y)|^2$  recorded exactly in the focal plane of the thin lens ( $d = f'$ ,  $O = F'$ ) coincides with the modulus square of the transverse Fourier

transform of  $A_0(x, y)$ . We will also examine how to calculate the transverse intensity profile of the beam in a plane “out of focus”, *i.e.* shifted from the focal plane ( $d = f' + \varepsilon$ ).

Considering optical wave propagation under the paraxial approximation, it can be easily shown (see [2] and Sec. 7 for details) that the transverse intensity profile found in a plane separated by a distance  $d$  from the lens reads :

$$|A_d(x, y)|^2 = \frac{1}{(\lambda d)^2} \times \left| \iint_{-\infty}^{+\infty} A_L(x', y') \exp\left[j\left(\frac{1}{d} - \frac{1}{f'}\right)\frac{k_0}{2}(x'^2 + y'^2)\right] \exp\left[-j\frac{k_0}{d}(xx' + yy')\right] dx' dy' \right|^2 \quad (4)$$

where the FT of  $A_L(x', y')$  is  $\tilde{A}_L(k_x, k_y) = \tilde{A}_0(k_x, k_y) \exp[-jd_0(k_x^2 + k_y^2)/(2k_0)]$ .

If a CCD camera is placed exactly in the focal plane of the lens ( $d = f'$ ,  $\varepsilon = 0$  in Eq. 4), it records an intensity profile  $|A_d(x, y)|^2$  that is proportional to the far field spectrum previously defined :

$$n(k_x, k_y) = (\lambda f')^2 \left| A_{f'}\left(x = \frac{f'}{k_0}k_x, y = \frac{f'}{k_0}k_y\right) \right|^2 \quad (5)$$

If the CCD camera is not exactly placed in the focal plane of the lens ( $d \simeq f'$  with  $d \neq f'$ ), the term  $\exp\left[j\left(\frac{1}{d} - \frac{1}{f'}\right)\frac{k_0}{2}(x'^2 + y'^2)\right]$  found in Eq. (4) plays a non-negligible role and the intensity pattern recorded by the CCD camera can significantly differ from the true far-field pattern recorded for  $d = f'$ . As described more in detail in Sec. 3, the differences between the transverse intensity pattern recorded by the CCD camera and the true far-field pattern increase when the third-order nonlinearity  $\chi^{(3)}$  increases.

Before describing more in details the influence of a mispositioning of the CCD camera, it is worth noticing that Eq. (5) does not depend on the distance  $d_0$  between the output side of the nonlinear medium and the lens when  $d = f'$  ( $\varepsilon = 0$ ). Our numerical calculations have shown that the transverse intensity profile recorded out of the focal plane ( $\varepsilon \neq 0$ ) depends slightly on the distance  $d_0$ . Therefore, for the sake of simplicity, we will not consider the influence of this additional parameter in this paper and we will restrict our analysis to the situation in which the output side of the Kerr medium is close to the lens ( $d_0 = 0$ ).

Passing through the Kerr medium, the beam acquires a nonlinear phase depending on the transverse coordinates. In this paper, we limit our theoretical work to the case of a thin nonlinear medium. Using the common approach to describe propagation through thin nonlinear media [53, 55–60], *we assume that light diffraction plays a negligible role in the nonlinear medium*. The length  $L$  of the Kerr medium is thus considered to be much smaller than the diffraction length. Under this assumption, the complex amplitude of the light field found at the output of the Kerr medium reads:

$$A_0(x, y) = A_{in}(x, y) \exp\left[j2\pi\gamma|A_{in}(x, y)|^2\right]. \quad (6)$$

$\gamma$  is given by  $\gamma = \chi^{(3)}LI_0/(2\pi)$  where  $\chi^{(3)}$  is third-order nonlinearity coefficient.  $|A_{in}|^2$  and  $|A_0|^2$  are normalized with respect to the maximum value of the optical intensity  $I_0$ .  $\chi^{(3)}$  is positive in media such as silica and it can be either positive or negative in photorefractive media.

### 3. Far field measurement of a gaussian beam with self-phase modulation

In this Sec. 3 we examine the impact of a mispositioning of the CCD camera on the measurement of the far-field profile of a gaussian beam having a waist  $w$ . The normalized amplitude of

the electric field at the input side of the nonlinear medium is :

$$A_{in}(x,y) = \exp\left(-\frac{1}{2}(x^2+y^2)/w^2\right) \quad (7)$$

The numerical value taken for the diameter  $2w$  of the gaussian beam is 3 mm (see Fig. 3(a)), which is representative of the experiments on optical wave turbulence carried out by Sun *et al* in ref. [48]. We will examine the influence of nonlinear phase shifts on the transverse structure of the light beam in a realistic way. In particular, in our numerical simulations, the maximum nonlinear phase shift taken by the light beam does not exceed  $2\pi$  ( $|\gamma| \leq 1$ ), which corresponds to values readily accessible in standard experiments made with cw lasers passing through liquid crystals or photorefractive crystals [23, 48]. In all this paper we use a numerical value of the focal length of the thin lens  $f' = 50\text{mm}$ .

All numerical calculations presented in Sec. 3, 4 and 5 have been performed with transverse grids having a square shape. In Sec. 3 and 4 the surface of the square is  $25 \text{ mm}^2$  ( $x, y \in [-5\text{mm}, 5\text{mm}]$ ). All the numerical computations presented in this paper have been performed with a large number of points ( $32,768 \times 32,768$  points) in order to avoid any sampling and/or boundary conditions artifacts (see Sec. 7).

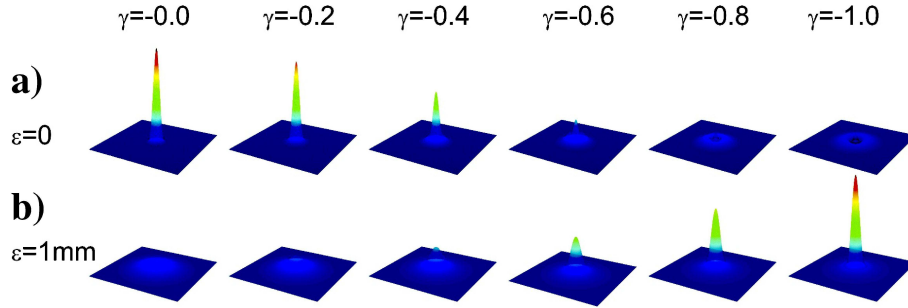


Fig. 2. (a) Far-field patterns observed exactly in the focal plane of the lens ( $\varepsilon = 0$ ) and (b) transverse “far-field” patterns observed slightly out of the focal plane ( $\varepsilon = +1\text{mm}$ ). The strength of nonlinearity is increased from  $\gamma = 0$  to  $\gamma = -1$  (defocusing self-phase modulation). The far-field observed exactly in the focal plane of the lens broadens as the nonlinearity increases. If the observation plane is slightly shifted ( $\varepsilon = +1\text{mm}$ ), the observed “far-field” narrows when the nonlinearity increases.

First considering that the observation screen or CCD camera is well positioned ( $d = f'$ ), we numerically compute the far field given by Eqs. (5), (6) and (7) for a lens having a focal length  $f' = 50\text{mm}$ . Fig. 2(a) shows the evolution of the far field pattern when the nonlinear coefficient  $\gamma$  is changed from zero to  $-1$  (defocusing self-phase modulation). The light beam experiences self-phase modulation and the far-field pattern thus undergoes a significant broadening when the nonlinearity increases. As shown in Fig. 2(a), the far field pattern exhibits concentric rings together with this spectral broadening. This phenomenon is very well known and it has been extensively studied experimentally and theoretically in the self-focusing and self-defocusing cases [11, 12, 49–52, 60]. Recently the influence of a nonlocal Kerr effect on the far field of a gaussian beam has also been considered [53]

Let us now examine the consequences of a slight mispositioning of the observation screen (CCD camera) and let us assume that it is slightly moved away from the lens, at a distance  $d = f' + \varepsilon$  ( $\varepsilon > 0$ ) slightly larger than  $f'$  (see Fig. 1). As shown in Fig. 2(b), keeping  $f' = 50\text{mm}$ , fixing  $\varepsilon = +1\text{mm}$  and changing the nonlinear coefficient  $\gamma$  from zero to  $-1$ , we now observe a narrowing of the spectrum recorded by the CCD camera instead of the broadening observed when the true far field is accurately measured (see Fig. 2(a)).

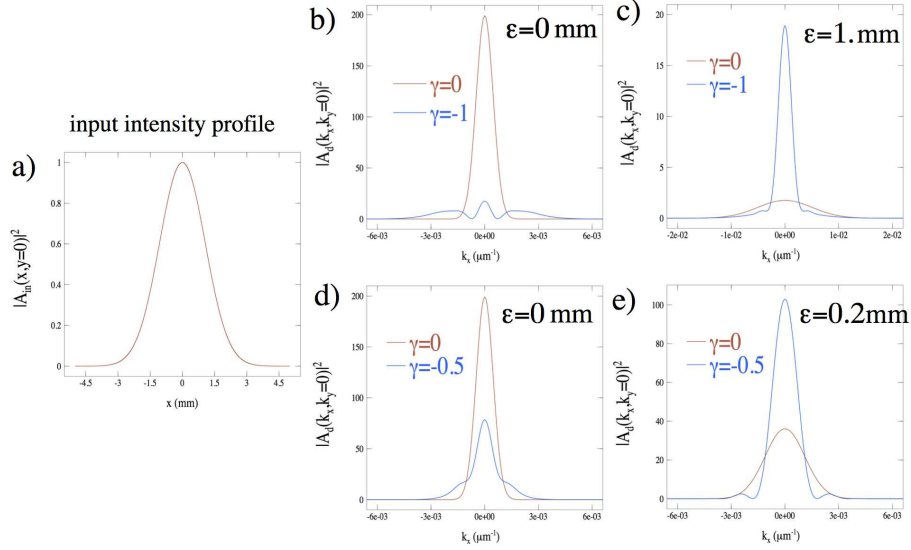


Fig. 3. *Transverse intensity profiles.* a) Input profile. b) and d) Far field observed exactly in the focal plane  $\epsilon = 0$  for a zero ( $\gamma = 0$ , red curve) and nonzero third order nonlinearity (blue curve b)  $\gamma = -1$  d)  $\gamma = -0.5$ ). c) and e) Corresponding transverse patterns observed slightly out of the focal plane. c)  $\epsilon = 1$ mm,  $\gamma = 0$  (red curve) and  $\gamma = -1$  (blue curve). e)  $\epsilon = 0.2$ mm,  $\gamma = 0$  (red curve) and  $\gamma = -0.5$  (blue curve).

Moving from a three-dimensional plotting to a two-dimensional plotting, Fig. 3 shows transverse intensity profiles (cross sections with  $y = 0$  or  $k_y = 0$ ) for some selected values of the mispositioning parameter  $\epsilon$  and of the nonlinearity coefficient  $\gamma$ . Fig. 3(a) represents the intensity profile  $|A_0(x, y = 0)|^2$  found at the output side of the nonlinear medium (near field intensity pattern). The curves plotted in red lines in Fig. 3(b), 3(c), 3(d), 3(e) represent profiles recorded at several positions of the CCD camera without nonlinearity ( $\gamma = 0$ ). The curves plotted in blue lines in Fig. 3(b), 3(c), 3(d), 3(e) represent profiles recorded by the CCD camera at the same positions but for two possible values of the Kerr coefficient ( $\gamma = -0.5$ ,  $\gamma = -1$ ). As already evidenced in Fig. 2, the spectrum narrows instead of broadening when  $|\gamma|$  increases. This phenomenon is very sensitive and it can be observed even for a very small shift of the camera out of the focal plane ( $f' = 50$  mm and  $\epsilon = +1$  mm in Fig. 3(c)). Fig. 3(e) shows that an error  $\epsilon$  in the position of the CCD camera as small as  $\epsilon = +200\mu\text{m}$  leads to the same spurious observation of a spectral narrowing instead of a spectral broadening.

It is possible to understand the phenomenon above reported from a simple description made in terms of thin lenses combination. Let us firstly remark that, with our numerical parameters ( $w = 3$  mm,  $\lambda = 532\text{nm}$ ), the diffraction (Rayleigh) length is  $\pi(2w)^2/\lambda \simeq 26$  m, which is much greater than any other length-scale involved in our problem. If we first ignore optical Kerr effect ( $\gamma = 0$ ), this means that the input beam can be considered as being nearly collimated and consequently, that the position of the minimum beam waist is located very close to the back focal plane of the lens.

On the other hand, if  $\gamma \neq 0$ , self-phase modulation of the gaussian beam inside the thin Kerr medium induces a Kerr-lens [54] having a focal length  $f'_{Kerr}$ .  $f'_{Kerr}$  can be evaluated from a first-

order Taylor expansion of Eq. (7) in  $(x^2 + y^2)/w^2$ . Under this approximation, Eq. (6) becomes :

$$A_0(x, y) = A_{in}(x, y) \exp(j2\pi\gamma) \exp\left[-j\gamma\pi(x^2 + y^2)/w^2\right] \quad (8)$$

The comparison between Eq. (8) and Eq. (16) found in Sec. 7 gives :

$$f'_{Kerr} = \frac{w^2}{\gamma\lambda}. \quad (9)$$

Still considering that  $d_0 = 0$  (see Fig. 1), the gaussian beam passes through an effective lens made up with two lenses placed side by side with focal lengths respectively of  $f'$  and  $f'_{Kerr}$ . The focal length of this effective lens is given by  $(f'_{eff})^{-1} = (f')^{-1} + (f'_{Kerr})^{-1}$ . In the examples above presented (see Fig. 2 and Fig. 3), the sign of the nonlinear coefficient is negative ( $\gamma \leq 0$ ) so that  $f'_{Kerr} \leq 0$  and thus  $f'_{eff} > f'$ . With  $f' = 50\text{mm}$  and  $\gamma = -1$  one gets  $f'_{Kerr} \simeq -4\text{m}$  and  $f'_{eff} = 50.6\text{mm}$ . Increasing the strength of the nonlinearity, the major consequence of the Kerr-lens effect is to push the minimum beam waist at a distance  $d = f'_{eff} > f'$  (i.e.  $\varepsilon > 0$ ) from the lens. Observing the transverse intensity pattern with a CCD camera whose position is fixed slightly out of the focal plane of the observation lens ( $d = f' + \varepsilon$ ,  $\varepsilon > 0$ ), the transverse diameter of the pattern decreases when  $|\gamma|$  increases, as illustrated in Fig. 2 and 3.

Using numerical simulations, we have explored wide ranges of parameters and the unexpected phenomenon of narrowing of the far-field pattern observed slightly out of the focal plane of the thin lens has been found to be robust. In particular, the value taken by  $d_0$  does not play any crucial role. Our numerical simulations also show that the evolution of the measured pattern (with  $\varepsilon \neq 0$ ) is non monotonic with  $\gamma$ . Increasing the value of  $\gamma$  from zero, the measured spectral width first decreases and then increases at high value of  $\gamma$ . Our numerical simulations show that identical behaviors are also observed for  $\gamma > 0$  and  $\varepsilon < 0$ .

This can be easily understood from the interpretation above given and based on the effective focal length  $f'_{eff}$ . Note that if  $\gamma$  and  $\varepsilon$  have identical sign, the width of the measured spectrum increases as expected but it strongly differs from the width of the true far-field spectrum. From the general point of view, *the error made in the measurement of the far field increases when the nonlinearity (self phase modulation) increases.*

In the phenomenon of wave condensation predicted from WT theory, the Fourier power spectrum (far-field) of an initially incoherent light wave narrows as the result of the turbulent nonlinear interactions among the waves [39, 40]. The phenomenon demonstrated in this paper has to be taken into account with great care in order to interpret results from experiments designed to observe the process of optical wave condensation [48].

In wave turbulence experiments tracking *e.g.* the wave condensation phenomenon, the initial condition is a incoherent *i.e.* random field [44, 45, 48]. In the Sec. 4, we explore the robustness of the unexpected narrowing of the measured far-field when strong phase noise is added to the gaussian field.

#### 4. Random initial condition

In Sec. 3, we have considered the propagation of a coherent gaussian beam passing through a Kerr-like medium with an infinite transverse size. We are now going to examine the nonlinear propagation of an initially incoherent (i.e. noisy) optical beam in the same setup (see Fig. 1). The situation under consideration is in its principle very similar to the archetype of an experiment designed to observe the phenomenon of 2D optical wave condensation [35, 38–40]. For instance, in experiments reported in [48], a gaussian beam passes through a spatial light modulator having a random transmission permitting to design an incoherent wave with an appropriate Fourier spectrum.

In this Sec. 4, we show that adding phase noise to the gaussian beam does not qualitatively change the unexpected phenomenon of far field narrowing described in Sec. 3.

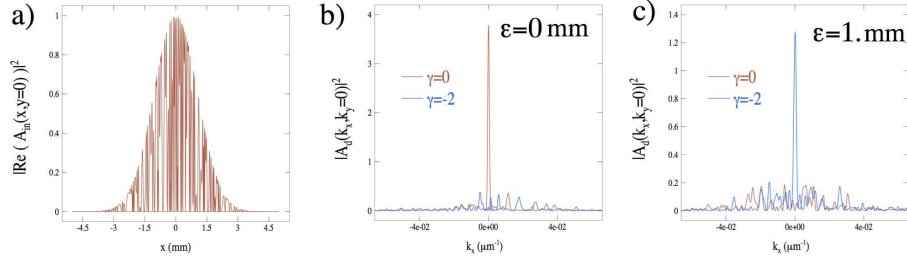


Fig. 4. *Random initial conditions* a) transverse intensity profile of the field at the entrance side of the Kerr medium  $|Re(A_{in}(x, y=0))|^2$  b) Far field observed exactly in the focal plane ( $\epsilon = 0$ ) for  $\gamma = 0$  (red curve) and  $\gamma = -2$  (blue curve) : the far-field broadens as the nonlinearity increases. c) Transverse patterns observed slightly out of the focal plane  $\epsilon = 1$ mm for  $\gamma = 0$  (red curve) and  $\gamma = -2$  (blue curve). Slightly out of the focal plane, the observed “far-field” narrows when the nonlinearity increases. This phenomenon is robustly preserved even if a strong phase noise is added to the initial condition.

To examine the nonlinear propagation of a spatially-incoherent beam, we replace the expression of the input gaussian amplitude given by Eq. (7) by

$$A_{in}(x, y) = \exp\left(-\frac{1}{2}(x^2 + y^2)/w^2\right) \exp(j\phi(x, y)) \quad (10)$$

where  $\phi(x, y)$  is a random phase. Fig. 4(a) represents the modulus square of the real part of  $A_{in}(x, y=0)$  *i.e.* of the incoherent wave launched inside the Kerr medium.

Keeping mispositioning parameter already used to compute Fig. 3(b) and 3(c) ( $\epsilon = 0$ mm,  $\epsilon = +1$ mm) and using  $\gamma = -2$ , we redo numerical simulations presented in Sec. 3 with this new initial condition. As in Sec. 4, we still use a transverse grid having a square shape ( $x, y \in [-5\text{mm}, 5\text{mm}]$ ) discretized by  $32768 \times 32768$  points. Fig. 4(b) represents the far-field patterns observed exactly in the focal plane of the lens with and without any nonlinearity (red and blue line respectively). In spite of the presence of noise, Fig. 4(b) reveals features qualitatively similar to those already reported in Fig. 3.b for the coherent gaussian beam : the far-field intensity pattern broadens when the strength of the nonlinearity is increased. Moving the observation plane slightly out of focus ( $\epsilon = +1$ mm), Fig. 4(c) shows the evolution of the transverse intensity pattern when the strength of the nonlinearity is increased. Note that we have observed behaviors that are qualitatively similar by changing the phase noise into intensity noise.

The presence of noise does not qualitatively change features already evidenced in Fig. 3(c) or 3(e): with a tiny error in the positioning of the detector, the observed intensity pattern narrows when  $|\gamma|$  is increased. This is a crucial result in the context of optical wave condensation experiments in which a speckle-like beam is launched inside a Kerr medium.

As an example, in some recent experiments made with a photorefractive crystal, the strength of nonlinearity can be experimentally controlled by the voltage applied to the crystal [48]. The authors have observed a pronounced narrowing of the intensity pattern recorded by the CCD camera when the strength of the nonlinearity is increased. They interpret this spectrum narrowing as the classical condensation of waves arising from the interplay of nonlinearity and diffraction [39]. Neglecting diffraction inside a pure thin Kerr medium, our calculations show that this narrowing phenomenon can be observed in a plane very close to the focal plane of a thin lens.

## 5. Finite-size effect of optical components

In Sec. 3 and 4, we have considered the propagation of coherent and incoherent gaussian beams passing through a Kerr-like medium having an *infinite* transverse size. In wave turbulence, Fourier spectrum is used in log scale and measured over many decades in order to observe power laws ; in particular, for systems described by nonlinear Schrödinger equations, the signature of wave thermalization is a power law  $k^{-2}$  for high transverse wavenumbers. We show in this Sec. 5 that the *finite* size of the nonlinear medium itself can significantly influence the shape of the tails of the intensity pattern recorded by the CCD camera in the setup shown in Fig. 1. We then comment the way through which the observation of the resulting transverse intensity pattern can possibly lead to some misinterpretations in experiments on thermalization of optical waves.

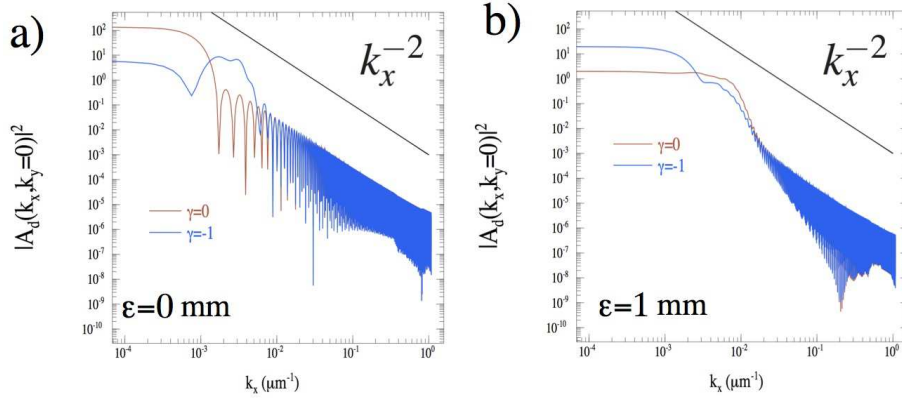


Fig. 5. Influence of the finite size of a square aperture. An input gaussian beam passes through the Kerr medium with a square section  $a \times a = 5 \times 5$  mm. Far field pattern observed (with log scale) : a) exactly in the focal plane of the lens ( $\epsilon = 0$  mm) b) slightly out of the focal plane ( $\epsilon = 1$  mm). Red curves :  $\gamma = 0$ . Blue curves :  $\gamma = -1$ . The phenomenon of unexpected narrowing of the spectrum is again observed for  $\epsilon = 1$  mm. One observes the signature of the Fourier transform of the square  $|\sin(k_x a/2)/(k_x a/2)|^2$ . Black curves :  $1/k_x^2$

We assume that the nonlinear bulk medium has a square section with 5mm-long sides. As in Sec. 3, we consider the nonlinear propagation of a coherent gaussian beam. The extension of the beam transverse profile is spatially limited and the input amplitude of the field  $A_{in}(x, y)$  described by equation (7) is now changed into:

$$A_{in, square}(x, y) = \text{rect}(x, y) \times A_{in}(x, y) \quad (11)$$

$$\text{with} \quad \text{rect}(x, y) = \begin{cases} 1 & \text{if } |x| \leq a \text{ and } |y| \leq a \\ 0 & \text{else} \end{cases} \quad \text{with } 2a = 5 \text{ mm} \quad (12)$$

Keeping parameters already used to compute Fig. 3(b) and 3(c) ( $\epsilon = 0$  mm,  $\epsilon = +1$  mm and  $\gamma = -1$ ), we redo numerical simulations presented in Sec. 3 with this new initial condition. As in Sec. 3, we still use a transverse grid having a square shape (but with  $x, y \in [-7.5 \text{ mm}, 7.5 \text{ mm}]$ ) discretized by  $32768 \times 32768$  points. Fig. 5(a) plotted in vertical logarithmic scale represents far-field patterns observed exactly in the focal plane of the lens ( $\epsilon = 0$  mm) with and without nonlinearity (red and blue lines respectively). Fig. 5(b) represents the transverse intensity pattern observed slightly out of focus ( $\epsilon = +1$  mm). As already evidenced in Sec. 3, Fig. 5(b) shows that the spectrum narrows instead of broadening when the strength of the nonlinearity increases.

However let us emphasize that the wings of the transverse intensity spectra decay according to a power law scaling as  $k_x^{-2}$  whatever the position of the CCD camera. This new feature arises from the diffraction of light onto the edges of the finite-size nonlinear medium. The origin of the power law observed and of the exponent  $-2$  can be easily understood from simple physical considerations. The Fourier transform of  $A_{in,square}(x,y)$  is the convolution of the Fourier transform of  $A_{in}(x,y)$  with the Fourier transform of  $rect(x,y)$  which is  $\widetilde{rect}(k_x,k_y) = (2a)^2 sinc(k_x a) sinc(k_y a)$ . Reminding that  $sinc(x) = \sin(x)/x$ , the maxima of the horizontal cross section of the power spectrum are proportional to  $1/k_x^2$ .

Although this decay of the wings of the spectra according to a power law can be straightforwardly interpreted from light diffraction onto the edges of the nonlinear medium, we emphasize that this behavior must be well kept in mind in optical wave turbulence experiments. Indeed a decay of a power spectrum according to a  $1/k^2$  law is the signature of the thermodynamical Rayleigh-Jeans distribution characterizing the equilibrium state reached by wave systems described by NLS equations [35, 38, 48].

Note that Rayleigh-Jeans distribution predicted by WT theory applied to the 2D nonlinear Schrödinger equation corresponds to a power law  $k^{-2} = |\mathbf{k}|^{-2}$  for high-frequency wavenumbers  $\mathbf{k}$  [35, 38]. For the sake of simplicity, an horizontal cross section of the spectrum is plotted in Fig. 5 as it seems to be done in [48]. The horizontal axis is therefore the  $k_x$  component of the wavenumber  $\mathbf{k}$ . Averaging all the cross sections over the isoline  $k = \sqrt{k_x^2 + k_y^2}$  in the  $\mathbf{k}$ -space gives a slightly modified power law for the spectrum  $n(k)$ . The main goal of this Sec. 5 is not an exhaustive study of this power law but to point out that diffraction effect may play crucial role in 2D WT experiments.

In all optical experiments, light diffraction onto the edges of crystals, mirrors or lenses may lead to this kind of decay obeying a power law. Therefore, wave turbulence experiments have to be designed with caution : the spectrum tails corresponding to the diffraction on all the edges found in the setup have to have a negligible weight relatively to awaited thermodynamical distribution.

## 6. Conclusion

In this paper, we have theoretically studied a conceptually-simple optical setup in which the far-field intensity pattern of a light beam passing through a Kerr medium is measured in the focal plane of a thin lens. Using Fresnel diffraction formula and usual theoretical models of thin lens and thin Kerr medium, we have investigated the influence of the nonlinear phase shift and of the distance between the lens and the detector.

We have shown that the transverse intensity pattern observed in the back focal plane of the thin lens dramatically depends on the longitudinal position the CCD camera. Although the “true” far field pattern is actually correctly measured when the CCD camera is exactly placed in the focal plane, significant deviations from the “true” far field pattern are observed even for a small mispositioning of the CCD camera. Those deviations have been shown to possibly occur in real-life optical systems, for light beams experiencing nonlinear phase shifts of the order of  $2\pi$ , and for errors in the position of the CCD camera as small as  $\sim 200\mu\text{m}$  or  $\sim 1\text{ mm}$  at focal lengths of  $\sim 50\text{ mm}$ . From the general point of view, the phenomenon reported in this paper may be at the origin of large uncertainties in the quantitative measurement of transverse wavenumbers and it may take some importance in various experiments devoted for instance to the study of pattern formation [23, 25] or dispersive shock waves [31, 34].

However, far beyond the existence of quantitative errors possibly made in some measurements, we have shown that a tiny mistake in the position of the CCD camera may lead to qualitatively-erroneous interpretations about the observed phenomena. Mispositioning the CCD camera by only  $\varepsilon \simeq 200\mu\text{m}$  behind a lens with a focal length of  $50\text{ mm}$  and increasing the non-

linear phase shift from 0 to  $\sim 2\pi$ , numerical simulations evidence a narrowing instead of the anticipated broadening of the transverse intensity pattern. This phenomenon has been demonstrated for a coherent gaussian beam (see Sec. 3) but it is robust enough to persist for incoherent beams strongly modified by the presence of a phase noise (see Sec. 4). We believe that this result is of significance in the context of optical experiments tracking the phenomenon of wave condensation [39, 40, 48]. Optical wave condensation is a classical phenomenon analogous to the bose Einstein condensation : its signature in 2D optical experiments is a narrowing of the Fourier (far-field) spectrum as the result of the interplay between diffraction and nonlinearity in the Kerr-like medium.

In addition with these problems related to the positioning of the CCD camera behind the lens, we have shown that WT experiments may suffer from another artefact. Wave condensation and energy equipartition among the modes (with high wavenumbers  $k$ ) are two phenomena arising from the same general wave thermalization process [39]. In 2D waves systems that are described by nonlinear Schrödinger equation, energy equipartition (characterizing the so-called Rayleigh-Jeans spectrum) corresponds to a power law  $k^{-2}$  in the far field pattern [35, 38, 39]. We have shown that the well-known transverse intensity patterns arising from light diffraction by the edges of the nonlinear medium may be wrongly interpreted as this Rayleigh-Jeans spectrum (see Sec. 5).

Recent works have shown that nonlinear optics is a field in which fundamental phenomena predicted by WT theory can be explored [38, 41, 44, 45, 48]. Phenomena such as wave thermalization, wave condensation or Kolmogorov-Zakharov cascades have clear signatures in the Fourier space [35]. In spatial optical experiments, the observation of the spectra of incoherent waves requires a far-field analysis. We have shown in this article that the observation of these phenomena in transverse nonlinear optics experiments is very challenging and that it requires great cares in the measurement of the far field spectrum.

Let us emphasize that those difficulties in the measurement of the transverse far field pattern are usually not found in optical experiments dealing with transverses patterns such as rolls or hexagons which have usually a finite number of transverse wavevectors [21, 23]. As a consequence, in the studies devoted to pattern formation, experimentalist may slightly adjust the position of the detector in order to observe sharp and discrete components in the far field. In the context of wave turbulence, the wave spectra are continuous and it is therefore hard to apply simple “eye-criteria” to align the setup.

Future experimental works will have to be done in order to observe the unexpected narrowing of the far field numerically predicted in this paper. Moreover, in future wave turbulence experiments in nonlinear optics, it is very important to go through the limitations described in this paper. In particular, highly sensitive methods have to be developed and used in order to adjust the relative position of the lens and of the detector. Transverse analysis of the phase and not only of the intensity of the beam could be helpful to align the optical setup.

## 7. Appendix: Fresnel diffraction and propagation through a thin lens

In this Sec. 7, we give a brief demonstration of Eq. (4). Eq. (4) gives the transverse intensity profile of a linearly polarized field in a plane located at a distance  $d$  from a thin lens with a focal length  $f'$  (see Fig. 1). We report the reader to [2] for a detailed demonstration.

In all this paper, we assume that the amplitude  $A(x, y, z)$  is a slowly-varying function of the longitudinal coordinate (*i.e.*  $k_0 |\partial_z A| \gg |\partial_{zz} A|$ ). Under this paraxial assumption, the usual propagation equation for a linearly-polarized electric field in vacuum ( $\partial_{tt} - c^2 \partial_{zz}$ )  $E = 0$  becomes:

$$\partial_z A = \frac{j}{2k_0} (\partial_x^2 + \partial_y^2) A \quad (13)$$

From Eq.(13), it is straightforward to show that the transverse Fourier transform of  $A(x, y, z)$  reads:

$$\tilde{A}(k_x, k_y, z) = \exp \left[ -\frac{j(k_x^2 + k_y^2)}{2k_0} z \right] \tilde{A}(k_x, k_y, z = 0) \quad (14)$$

where  $\tilde{A}(k_x, k_y, z = 0)$  is the transverse Fourier transform of  $A(x, y, z = 0)$ .

Using the inverse Fourier transform, we get the so-called *Fresnel diffraction* formula :

$$A(x, y, z) = \frac{1}{j\lambda z} \iint_{-\infty}^{+\infty} A(x', y', z' = 0) \exp \left[ j \frac{\pi}{\lambda z} ((x - x')^2 + (y - y')^2) \right] dx' dy' \quad (15)$$

Propagating through a thin positive lens used in Gauss conditions (*i.e.* in paraxial approximation), let us recall that the electric field acquires a quadratic phase [2] so that:

$$A'_L(x, y) = A_L(x, y) \exp \left[ -j \frac{\pi}{\lambda f'} (x^2 + y^2) \right] \quad (16)$$

where  $A_L$  is the input field in the front plane of the lens,  $A'_L$  is the field just after the the lens and  $f'$  is the focal length of the lens, .

As considered in Fig. 1, the field  $A(x, y, z)$  first propagates over a distance  $d_0$ , then pass through a lens with a focal lens  $f'$  and finally propagates over a distance  $d$  (before reaching the screen or the camera). Combining Eq. (15) and (16) one gets :

$$A_d(x, y) = \frac{1}{j\lambda d} \exp \left[ j \frac{\pi}{\lambda d} (x^2 + y^2) \right] \times \iint_{-\infty}^{+\infty} A_L(x', y') \exp \left[ j \left( \frac{1}{d} - \frac{1}{f'} \right) \frac{\pi}{\lambda} (x'^2 + y'^2) \right] \exp \left[ -j \frac{2\pi}{\lambda d} (xx' + yy') \right] dx' dy' \quad (17)$$

If  $d = f'$ ,  $A_d(x, y)$  is proportionnal to the Fourier transform of  $A_L$  and finally one gets :

$$|A'_{f'}(x, y)|^2 = \frac{1}{(\lambda f')^2} |\tilde{A}_L(k_x, k_y)|^2 \text{ with spatial wavenumbers } k_x = \frac{2\pi x}{\lambda f'} \text{ and } k_y = \frac{2\pi y}{\lambda f'} \quad (18)$$

where  $\tilde{A}_L(f_x, f_y)$  is given by Eq. (14) with  $z = d_0$ ,  $A(x, y, z = 0) = A_0(x, y)$  and  $A(x, y, z = d_0) = A_L(x, y)$ . Using  $|\tilde{A}_L(k_x, k_y)|^2 = |\tilde{A}_0(k_x, k_y)|^2$  and considering the field exactly in the focal plane of the lens  $A_{d=f'}(x, y)$  one finally gets :

$$|A_{f'}(x, y)|^2 = \frac{1}{(\lambda f')^2} |\tilde{A}_0(k_x, k_y)|^2 \quad (19)$$

Notice that the intensity far field pattern  $|A_{f'}(x, y)|^2$  does not depend on the propagation distance  $d_0$  between the initial plane ( $O', x', y'$ ) and the lens.  $d_0$  only affects the transverse phase of  $A_{f'}(x, y)$ .

In the numerical simulations, the propagation in free space is computed in the Fourier space with the FFT routine FFTW [61] and the equation (14). On the contrary, we compute the field passing through a lens in the direct space from Eq. (16). The boundary conditions are periodic on our square grid. As suggested by equation (19) and as it would be done in experiments, we finally multiply the intensity pattern  $|A_d(x, y)|^2$  by the constant  $(\lambda f')^2$  in order to get the spectral power density in the Fourier space.

Along the propagation, the beam experiences strong changes in its typical diameter. The beam diameter varies from a few millimeters in the input plane ( $w = 3\text{mm}$ ) to  $10\mu\text{m}$  in the focal plane of the lens. In order to avoid sampling problem we have used a large number of points with a grid of  $32768 \times 32768$  points. We have carefully checked the accuracy of numerical computations (in particular those represented in log scale in Fig. 5) by varying the number of points and the size of the window ( $5 \times 5\text{mm}$  in Sec. 3, 4 and 5 and  $7.5 \times 7.5\text{mm}$  in Sec. 5).

Finally, notice that when the circular symmetry is preserved, it is possible to simplify the equation (17).  $A_L(x', y')$  is replaced by  $A_L(r)$  where  $r = \sqrt{x'^2 + y'^2}$ . Using Bessel functions properties we get :

$$|A_d(x, y = 0)|^2 = \frac{1}{(\lambda d)^2} \left| \int_{-\infty}^{+\infty} A_L(r) \times \exp\left[j\left(\frac{1}{d} - \frac{1}{f'}\right)\frac{\pi}{\lambda} r^2\right] \times J_0\left(\frac{2\pi r x}{\lambda d}\right) \times 2\pi r dr \right|^2 \quad (20)$$

where  $J_0(X)$  is the first kind modified Bessel function of order 0. This formula can be applied only to examples of Sec. 3 (circular symmetry) but not to the cases of Sec. 4 and 5 which require 2D calculations.

### Acknowledgment

The authors thank Serge Bielawski for fruitful discussions and computing facilities and Elise Berrier for the nice 3D picture. The authors are grateful to Guy Millot for fruitful discussions. The Laboratoire de Physique des Lasers Atomes et Molécules is Unité Mixte de Recherche 8523 of th CNRS. This work was supported by the Centre Européen pour les Mathématiques, la Physique et leurs Interactions (CEMPI).